Atmospheric
Measurement
Techniques
Open Access

Discussions

Retrieval of $\delta^{18}O$ and δD in atmospheric water vapour from ground-based FTIR

N. V. Rokotyan[1], V. I. Zakharov[1], K. G. Gribanov[1], F.-M. Bréon[2], J. Jouzel[2], R. Imasu[3], M. Werner[4], M. Butzin[4], C. Petri[5], T. Warneke[5], and J. Notholt[5]

[1]Laboratory of Climate and Environmental Physics, Ural Federal University, Russia
[2]Institut Pierre Simon Laplace, Laboratoire des Sciences du Climat et de l'Environnement, France
[3]Atmosphere and Ocean Research Institute, University of Tokyo, Japan
[4]Alfred Wegener Institute for Polar and Marine Research, Germany
[5]Institute of Environmental Physics, Bremen University, Germany

Correspondence to: N. V. Rokotyan (nrokotyan@gmail.com)

Discussion Paper | Discussion Paper | Discussion Paper | Discussion Paper

AMTD

7, 195–231, 2014

Retrieval of $\delta^{18}O$ and δD in atmospheric water vapour from ground-based FTIR

N. V. Rokotyan et al.

Title Page

Abstract	Introduction
Conclusions	References
Tables	Figures

|◄ | ►|
◄ | ►
Back | Close

Full Screen / Esc

Printer-friendly Version

Interactive Discussion

Abstract

This paper investigates the possibility of retrieving isotopic composition of atmospheric water vapour from high-resolution ground based measurements of atmospheric transmittance spectra in the near-infrared region (4000–11 000 cm^{-1}).

Simulated measurements of atmospheric transmittance were analyzed in order to find clear spectral signatures of H$_2^{18}$O, HDO and H$_2^{16}$O. Appropriate signals of the species of interest were found and also identified in measured spectra recorded by ground-based Fourier transform infrared spectrometer (FTIR) at the Institute of Environmental Physics of Bremen University. A set of H$_2^{18}$O, HDO and H$_2^{16}$O spectroscopic windows is presented.

Theoretical estimations of the retrieval precision indicate that spectra recorded by ground-based FTIR spectrometers can be used to measure the seasonal cycle of δ^{18}O and δD in the atmosphere. Studying the influence of the a priori on retrieval results shows low sensitivity to a priori assumptions. Impact of the uncertainties in spectroscopic line parameters of water isotopologues on precision of the retrieval of δ^{18}O and δD is investigated.

Time series of δ^{18}O retrieved from ground-based FTIR spectra are represented for the first time. Comparison with the results of ECHAM5-wiso isotopic general circulation model simulations demonstrates a good agreement for "summer" measurements. Conversely, the comparison of "winter" measurements and modeling result show a discrepancy that demonstrate worse agreement that may be connected with incorrect temperature dependence of spectroscopic parameters.

1 Introduction

Monitoring of isotopic content of water vapour provides a rich information on the water cycle. Heavier water isotopologues, HDO and H$_2^{18}$O, condense more actively and evaporates less actively than the main isotopologue H$_2^{16}$O. Each cycle of evaporation

Title Page

Abstract	Introduction
Conclusions	References
Tables	Figures

◀ | ▶▶

◀ | ▶

Back | Close

Full Screen / Esc

Printer-friendly Version

Interactive Discussion

and condensation generally results in depletion of the air of δ^{18}O and δD with increasing depletion as the water vapor mixing ratio, and thus the air mass temperature, decreases. This depletion process affects both δ^{18}O and δD with however subtle differences owing to the existence of an additional kinetic effect resulting from the differences in the diffusivity of water molecules in air. In turn, the isotopic composition of water vapour (either δ^{18}O or δD) can be used for understanding the atmospheric water cycle while co-isotopic measurements (δ^{18}O and δD) can shed light on kinetic processes associated with evaporation and condensation processes (Jouzel et al., 1987; Hoffmann et al., 1998; Noone et al., 2002; Yoshimura et al., 2008; Risi et al., 2010a, b; Werner et al., 2011).

Usually concentration ratio of different isotopologues is expressed in terms of delta-values:

$$\delta^x A = \left(\frac{(n_x/n_a)_{\text{sample}}}{(n_x/n_a)_{\text{standard}}} - 1 \right) \cdot 1000 \ [\text{‰}], \tag{1}$$

where $(n_x/n_a)_{\text{sample}}$ is a measured ratio of less abundant isotopologue to the most abundant, and $(n_x/n_a)_{\text{standard}}$ is a standard ratio. The Vienna Standard Mean Ocean Water (VSMOW) values are 2005.2×10^{-6} for ^{18}O/^{16}O and 155.76×10^{-6} for D/H (Craig, 1961). A commonly used approach for inferring information from δ^{18}O and δD co-isotopic measurements is through the deuterium-excess defined by Dansgaard (1964) as $d = \delta$D$ - 8 \cdot \delta^{18}$O.

Thanks to the recent development of methods allowing retrieval of information on the distribution of water isotopologues in the atmosphere there is a growing interest for using isotopic data for investigating atmospheric processes controlling tropospheric humidity and stratosphere–troposphere water vapour exchange (Rinsland et al., 1991; Moyer et al., 1996; Coffey et al., 2006; Payne et al., 2007).

Due to the difficulty of retrieving information about δ^{18}O in atmospheric water vapor, such studies are largely based on deuterium data. Satellite data from different instruments offer complementary information. While ACE and MIPAS give access to δD from

the stratosphere to the upper troposphere (Risi et al., 2012a, b), TES enables the retrieval of some information on the δD vertical distribution (Worden et al., 2006, 2007), IASI allows to retrieve δD in the mid troposphere, between 1 and 5 km (Pommier et al., 2013), and SCIAMACHY (Frankenberg et al., 2009) and GOSAT (Boesch et al., 2013; Frankenberg et al., 2013) provide with δD data integrated over the entire atmospheric column.

ATMOS Fourier transform infrared spectrometer installed on the Space Shuttle was the first instrument used to retrieve information about stratospheric abundances of $H_2^{18}O$, HDO, $H_2^{16}O$ and their ratios (Rinsland et al., 1991; Coffey et al., 2006). Actively developing satellite remote sounding techniques made it possible to obtain spatial and temporal distribution of δD in the troposphere by a posteriori δD calculations from retrieved $H_2^{16}O$ and HDO concentrations (Gribanov and Zakharov, 1999; Zakharov et al., 2004; Herbin et al., 2007, 2009; Frankenberg et al., 2009, 2013; Boesch et al., 2013) and by applying optimal estimation strategy to retrieve δD, which produces results not affected by different vertical sensitivities to $H_2^{16}O$ and HDO (Worden et al., 2006, 2007; Schneider and Hase, 2011). The first attempts to obtain tropospheric $\delta^{18}O$ from space were made by (Herbin et al., 2007) using IMG/ADEOS spectra in thermal IR region. However, satellite measurements cannot provide sufficient accuracy and precision to get temporal variations of $\delta^{18}O$ in the atmosphere. Remote sensing of δD from ground-based FTIR instruments was pioneered by Schneider et al. (2006, 2010, 2012) in the thermal infrared and now is under development in the near infrared (Gribanov et al., 2011; Skorik et al., 2013). Routine monitoring of atmospheric $\delta^{18}O$ is limited to in-situ measurements of water vapour isotopic composition at surface and analysis of precipitation samples (Rozanski et al., 1992; Kerstel et al., 1999; Lee et al., 2005; Steen-Larsen et al., 2013).

Ground-based FTIR remote sounding of atmospheric constituents is now actively used for validation of satellite data and long-term local measurements of the atmospheric composition. High spectral resolution of such instruments allows to clearly resolve absorption lines of atmospheric species with a good signal to noise ratio suitable

Title Page

Abstract | Introduction

Conclusions | References

Tables | Figures

◄ | ►

◄ | ►

Back | Close

Full Screen / Esc

Printer-friendly Version

Interactive Discussion

to monitor the atmospheric composition. Total Carbon Column Observing Network (TC-CON) (Wunch et al., 2010, 2011) and the Network for the Detection of Atmospheric Composition Change (NDACC) (Hannigan et al., 2009) are using FTIR observations for accurate and precise retrieval of CO_2, CH_4, H_2O, O_3, HF, HCl, and other gases con-

5 centration in the atmosphere. Retrieval of atmospheric methane, carbon dioxide and water vapour concentrations from ground-based high-resolution FTIR measurements is a routine procedure that could be done with precision up to 0.25 % (Wunch et al., 2011). TCCON community also produces standard products of HDO and $H_2^{16}O$ columnar values, which are often used for a posteriori δD calculations. Though such δD

10 calculations can be affected by different vertical sensitivity of $H_2^{16}O$ and HDO retrievals (Schneider and Hase, 2011), these data were successfully used for intercomparison with LMDZ-iso general circulation model simulations (Risi et al., 2012a, b) and GOSAT satellite retrievals (Boesch et al., 2013; Frankenberg et al., 2013). Within the MUSICA project measurements from ten NDACC stations were used for the optimally estimated

15 retrieval of δD vertical distribution in the troposphere (Schneider et al., 2012). These studies show that a growing network of ground-based FTIR sites is prospective for monitoring of the isotopic content of water vapour in the atmosphere.

In this article we focus on the retrieval of information about water isotopologues using ground-based FTIR measurements in near infrared. As SCIAMACHY and GOSAT, this

20 technique gives access to integrated column data and is thus mainly sensitive to the lower troposphere since about 90 % of the atmospheric water is below 500 hPa. Such lower tropospheric data are interesting to understand GCM biases in simulating the water cycle by models equipped with water isotopologues. Using the isotopic version of the LMD model, Risi et al. (2013) have investigated the role of continental recycling,

25 while Gryasin et al. (2013) has suggested that the difficulty of this model in simulating the water cycle over Western Siberia may be due to a problem in the large-scale advection or to insufficient surface evaporation. Also interesting is the fact that, at least in a model world, the δD of the total water column is highly correlated with δD near surface values as shown by Gribanov et al. (2013) for a site in Western Siberia. In turn,

such recent studies point both to the usefulness of total column integrated δD, which could be easily extended to the study of seasonal and intraseasonal variations when sufficient long time series will be available, and to the possibility of comparing and possibly combining such data with in-situ δD measurements in ground level water vapor at sites like Kourovka (Gribanov et al., 2013) where both FTIR and PICARRO measurements are performed. Obviously, getting reliable δ^{18}O data would further increase the interest of retrieving total column integrated water isotopologues using FTIR. If sufficient accuracy of the retrieved values of both isotopologues can be achieved one could for example get information about the oceanic origin of an air mass as its water vapor deuterium-excess is influenced by the conditions (humidity, temperature) prevailing in the evaporative source regions (Merlivat and Jouzel, 1979).

2 Spectral simulations and window selection

2.1 Spectral simulations

Though there are known H_2^{16}O and HDO spectral windows in near infrared region, which are used by TCCON community, we decided to look for additional ones that may improve the precision of δD calculations. As for our knowledge on H_2^{18}O, there are no reported windows in near infrared region that can be used for the isotopic retrieval.

To perform spectral windows selection we have simulated atmospheric transmittance spectra in wide spectral range from $4000\,\mathrm{cm}^{-1}$ to $11\,000\,\mathrm{cm}^{-1}$ by the FIRE-ARMS (Fine Infra-Red Explorer for Atmospheric Remote MeasurementS) software package (Gribanov et al., 1999, 2001) using a middle latitude summer standard model for atmospheric state (Anderson et al., 1986). These simulations were then analyzed to identify a number of spectral windows that contain clear signatures of H_2^{16}O, H_2^{18}O and HDO with little interference by absorption lines linked to other gases.

2.2 Spectral windows refinement

We have used GGG (ver.2012) software package (Wunch et al., 2011) to retrieve columnar concentrations of $H_2^{16}O$, $H_2^{18}O$ and HDO from the selected spectral windows from spectra recorded at Bremen TCCON site during 2010–2012 yr. We have analyzed retrieval results from measurements taken in different conditions: various humidity levels, wide atmospheric temperature range (summer and winter measurements), different solar zenith angles. We have used the following criteria for the spectral windows set refinement: (a) peak value in average fitting residuals shouldn't exceed 1.5 %; (b) correlation between columnar concentrations retrieved from different windows should be higher than 0.9. Refined HDO and $H_2^{16}O$ spectral windows set were then combined with those used in TCCON community. Usage of additional windows in our retrievals allowed us to improve the accuracy of the a posteriori calculated δD values by 25 % (comparing to the model). Thus the standard deviation of the difference between monthly averaged values of the calculated δD and simulated δD has improved from 24‰ to 18‰.

An example of retrieved scaling factors of a priori assumption for refined $H_2^{18}O$ windows is presented in Fig. 1. It should be noted that systematic shifts in retrievals are most likely caused by uncertainties in spectroscopic line intensities and half widths. The full set of refined $H_2^{16}O$, $H_2^{18}O$ and HDO windows is presented in Fig. 2 (see Table 1 for summarized information).

2.3 Measurement noise and retrieval precision

The FTIR instrument, which is used here, has signal-to-noise ratio (SNR) of 200 and 900 in selected $H_2^{18}O$ and HDO windows, respectively. To check if routine ground-based FTIR measurements are applicable for the retrieval of water vapour isotopic ratios, we have assessed the impact of the measurement noise on the retrieval (see Fig. 3). Because there are other sources of uncertainty, this analysis provides a lower estimate of the retrieval precision.

For such estimation atmospheric transmittances were simulated by FIRE-ARMS software in the selected spectral windows with the constant vertical profiles of $-15\,‰$ for δ^{18}O and $-200\,‰$ for δD, which are in range of natural atmospheric abundances of $H_2^{18}O$ and HDO. Normally distributed noise of different magnitudes representing different noise levels was added to the simulated spectra to imitate real measurements. Then the retrieval of δ^{18}O and δD was performed with only one fitting parameter: the scaling factor of the a priori profile of the isotopologue. As an a priori profiles initial profiles of the simulation perturbed by a random factor uniformly distributed in the range of 0.5–1.5 were used. This procedure was performed 100 times for each noise level.

Influence of the uncertainty of vertical temperature profile has also been analyzed. Perturbation in 1 % (2–3 K depending on altitude) in the temperature profile leads to approximately 3‰ and 10‰ deviation in the retrieved δ^{18}O and δD values, respectively.

2.4 Spectroscopic error sources

Along with measurement noise and temperature profile uncertainty, which represent random error of the retrieval, there are other error sources that introduce systematic impacts on the retrieved values. The retrieval procedure relies on spectroscopic data while uncertainties in water vapour spectroscopy remain an important problem (Rothman et al., 2013). Errors in line intensity and half widths reveal mainly in systematic shifts of the retrieved data while errors in the coefficient of temperature dependance of air-broadened half width effects the retrieval differently depending on atmospheric temperature. According to indices of uncertainty in HITRAN 2008 (Rothman et al., 2009), uncertainties in the intensity of water vapour spectral lines ranges from 5 to 10 % (that is about 50–100‰ in terms of delta-values) while uncertainty in air broadening coefficients typically ranges between 2 and 5 %. Uncertainty in the coefficient of temperature dependence of air-broadened half-width ranges between 10 % and 20 % and may introduce a bias that depends on atmospheric temperature. This error can lead to tangible under- or overestimation of concentration of the species of

interest from measurements taken in winter season when atmospheric temperatures are much colder than HITRAN reference temperature. An example of the influence from the coefficient of temperature dependence change by 15 % on $H_2^{18}O$ concentration as a function of atmospheric temperature is shown in Fig. 4. A small change in concentration of only one isotopologue of 0.5 % can lead to a change in delta values of about 4–5 ‰. Taking into account that in calculation of a delta-value participate two isotopologues and that uncertainty range of the coefficient of temperature dependence is relatively high (10–20 %), error in retrieved delta-values can be significant.

In the present study, we used modified GGG linelist (which is based on HITRAN 2008) (Wunch et al., 2010) with H_2O lines substituted by UCL08 water linelist (Shillings et al., 2011) because it provides us with better residuals and better agreement with the model. UCL08 is a compilation of experimental data (Jenouvrier et al., 2007; Mikhailenko et al., 2007, 2008; Coudert et al., 2008; Tolchenov and Tennyson, 2008), HITRAN2008 and additional theoretical lines (Barber et al., 2006). Strong lines of the isotopologues that are used in the retrieval of $\delta^{18}O$ and δD are identical to HITRAN2008.

As expected, retrieved columnar $\delta^{18}O$ and δD values are shifted from the columnar values calculated by the model (most likely due to uncertainties in line intensities and broadening parameters). We have calculated and corrected the offsets of 58 ‰ and −23 ‰ between retrieved and modeled $\delta^{18}O$ and δD correspondingly.

The HITRAN2012 (Rothman et al., 2013), which was recently made available, declares more accurate spectroscopic line intensities and half widths. Retrieval results obtained with this new version of HITRAN database have smaller systematic shifts from the model (+7 ‰ and −8 ‰ for $\delta^{18}O$ and δD, respectively) than those obtained with our GGG+UCL08 line list. Conversely, the correlation is smaller and the slope between retrieved and simulated isotopic ratios is further from the expected. These results indicate that improvement in the spectroscopic line parameters has a mixed impact on the isotopic retrievals and therefore needs further investigation.

Title Page

Abstract | Introduction

Conclusions | References

Tables | Figures

◄◄ | ►►

◄ | ►

Back | Close

Full Screen / Esc

Printer-friendly Version

Interactive Discussion

3 Instrumental and retrieval set-up

Since we investigate the feasibility of the retrieval of relative isotopic ratios of water vapour isotopologues from ground-based FTIR measurements in near-infrared that are widely collected by TCCON network we employed standard TCCON approach for this task. IR spectral measurements of the cloudless atmosphere registered at the Institute of Environmental Physics (IUP) of the University of Bremen (Germany, 53.104° N, 8.850° W, altitude 27 m, http://www.iup.uni-bremen.de) in 2009–2012 were used. IUP is the TCCON site that performs IR measurements in near-infrared region (4000–11 000 cm^{-1}) with resolution of 0.02 cm^{-1}. The operating FTIR instrument is a Bruker IFS-125HR with maximum resolution of 9×10^{-4} cm^{-1}. Measurements are collected in DC mode and then processed by a special software to reduce the impact of solar intensity variations caused by cloud and aerosol cover (Keppel-Aleks et al., 2007).

In general, retrieval of atmospheric parameters from measured spectra is an ill-posed inverse problem with non-uniqueness and unstable solution (Rodgers et al., 2000). The retrieval algorithm implemented in GGG package is based on minimization of the cost function J:

$$J = \sum_i \frac{(y_i - F(\alpha, \beta, v_i + \delta, \gamma_1 \boldsymbol{x}_1, \cdots, \gamma_m \boldsymbol{x}_m))^2}{\sigma_i^2}, \tag{2}$$

where F is the spectrum calculated by the forward model, y_i is the measured spectrum at the ith spectral channel, α and β are the continuum level and tilt values, v_i is the frequency wavenumber at the ith spectral channel, δ is the frequency shift of measured spectrum, $\gamma_1, \cdots, \gamma_m$ and $\boldsymbol{x}_1, \cdots, \boldsymbol{x}_m$ are the scaling factors and the a priori profiles of the gases that are being fitted correspondingly, σ_i is the uncertainty of the ith element in y. GGG uses scaling retrieval approach, which means that the a priori profile is scaled by the retrieved factor. As a consequence, the retrieval procedure makes no attempt at correcting the vertical profile, and only the total number of molecules of species of interest is sought. According to Wunch et al. (2011) such approach is much faster

than profile retrieval and less sensitive to some systematic errors in the shapes of the calculated spectral lines. Total number of molecules in atmospheric column is retrieved separately for $H_2^{16}O$, $H_2^{18}O$ and HDO and then delta values are calculated.

An example of weighting functions for $H_2^{18}O$ and HDO is shown in Fig. 5 (weighting functions in the other spectral windows behave the same). This illustrates that the method is mostly sensitive to the lower troposphere.

Since GGG package implements scaling retrieval algorithm, the shape of a priori profile can play an important role in accuracy of the retrieval. Initial guess profiles for $H_2^{16}O$ are derived from data of National Centers for Environmental Prediction and the National Center for Atmospheric Research (NCEP/NCAR) (Kalnay et al., 1996). HDO a priori profiles are calculated from $H_2^{16}O$ a priori profiles using the following equation (implemented in GGG package):

$$x_{HDO}^{apr}(h) = 0.16 \cdot x_{H_2^{16}O}^{apr}(h) \cdot \left(8.0 + \log_{10} \left(x_{H_2^{16}O}^{apr}(h) \right) \right), \tag{3}$$

where $x_{HDO}^{apr}(h)$ is the a priori HDO volume mixing ratio (vmr) profile, $x_{H_2^{16}O}^{apr}(h)$ is the a priori $H_2^{16}O$ vmr profile, h is the altitude. The term $0.16 \cdot \left(8.0 + \log_{10}(x_{H_2^{16}O}^{apr}(h)) \right)$ generally ranges between 0.40 (in the stratosphere) and 0.95 (in the troposphere) and qualitatively describes vertical depletion of HDO. The Eq. (3) applied to the simulations of ECHAM5-wiso isotopic general circulation model (see further below for a model description) approximates δD profiles with a standard deviation of about 35‰ in the lower troposphere.

To get $H_2^{18}O$ initial guess profiles we analyzed output of the ECHAM5-wiso model for the shapes of $\delta^{18}O$ isotopic profiles and found that $H_2^{18}O$ profile can be approximated as follows:

$$x^{\text{apr}}_{\text{H}_2^{18}\text{O}}(h) = 0.923 \cdot x^{\text{apr}}_{\text{H}_2^{16}\text{O}}(h) \cdot \left(\frac{x^{\text{apr}}_{\text{H}_2^{16}\text{O}}(h)}{x^{\text{apr}}_{\text{H}_2^{16}\text{O}}(h_{\text{trop}})} \right)^{\frac{8}{1000}} , \qquad (4)$$

where $x^{\text{apr}}_{\text{H}_2^{18}\text{O}}(h)$ is the a priori vmr profile of H_2^{18}O and $x^{\text{apr}}_{\text{H}_2^{16}\text{O}}(h_{\text{trop}})$ is the vmr value

of H_2^{16}O in the tropopause. Similar to Eq. (3) the term $0.923 \cdot \left(\frac{x^{\text{apr}}_{\text{H}_2^{16}\text{O}}(h)}{x^{\text{apr}}_{\text{H}_2^{16}\text{O}}(h_{\text{trop}})} \right)^{\frac{8}{1000}}$ ranges

between 0.90 and 0.99 and describe H_2^{18}O vertical depletion. Although this approach is
based on a limited number of simulations, it is certainly better than assuming a constant
vertical profile of the isotopic relative concentration. According to the model the Eq. (4)
describes $\delta^{18}\text{O}$ vertical profile with a standard deviation of 4 ‰ in the lower troposphere
(vs. 9 ‰ when using constant vertical profile). Standard GGG a priori profiles (Wunch
et al., 2010) were used as initial guess for other atmospheric species. Examples of
H_2^{16}O, $\delta^{18}\text{O}$ and δD a priori profiles are shown in Fig. 6.

To check the sensitivity of the retrieval to the shape of a priori profiles of $\delta^{18}\text{O}$ and δD
we performed a retrieval run using constant $\delta^{18}\text{O}$ and δD a priori profiles of 0 ‰ on the
same set of measurements. This test shows that, generally, retrieval is insensitive to
the initial guess. Standard deviation between the results of two different runs is about
0.5 ‰ for $\delta^{18}\text{O}$ and 3.8 ‰ for δD. This means that most of the retrieved information
about columnar values of $\delta^{18}\text{O}$ and δD comes from spectra and not from a priori
assumptions (Fig. 7).

As mentioned above, the retrieval employs model results from atmospheric simula-
tions using ECHAM5-wiso (Werner et al., 2011), which is the isotope-enhanced version
of the atmospheric general circulation model ECHAM5 (Roeckner et al., 2003, 2006;
Hagemann et al., 2006). The model considers both stable water isotopologues H_2^{18}O
and HDO which have been explicitly implemented into its hydrological cycle (Werner

et al., 2011), analogous to the isotope modeling approach used in the previous model releases ECHAM3 (Hoffmann et al., 1998) and ECHAM4 (e.g. Werner et al., 2001). For each phase of "normal" water (vapor, cloud liquid, cloud ice) being transported independently in ECHAM5, a corresponding isotopic counterpart is implemented in the model code. Isotopologues and "normal" water are described identically in the GCM as long as no phase transitions are concerned. Additional fractionation processes are defined for the water isotope variables whenever a phase change of the "normal" water occurs in ECHAM5, considering equilibrium and non-equilibrium fractionation processes.

ECHAM5-wiso has been validated with observations of isotope concentrations in precipitation and water vapor (Langebroeck et al., 2011; Werner et al., 2011; Gribanov et al., 2013). On a global and European scale, annual and seasonal ECHAM-5-wiso simulation results are in good agreement with available observations from the Global Network of Isotopes in Precipitation, GNIP (IAEA-WMO, 2006). The simulated near-surface isotopic composition of atmospheric water vapor is also in fairly good agreement with recent monthly observations from five different GNIP stations and with a continuous isotope record at Kourovka Observatory, Western Siberia. Model values and measurements agree well with differences in the range of ±10‰. A comparison of ECHAM5-wiso results with total column averages of HDO determined by the SCIA-MACHY instrument on board the environmental satellite ENVISAT (Frankenberg et al., 2009) shows the same latitudinal gradients, but an offset between 20–50‰ of unknown origin.

In this study, the horizontal model resolution is T63 in spectral space (about 1.9° × 1.9°), and model results for Bremen are evaluated at the nearest grid point. Vertical resolution is 31 levels on hybrid sigma-pressure coordinates. The model is forced with prescribed values of present-day insolation and greenhouse gas concentrations (IPCC, 2000), as well as with sea-surface temperatures and sea-ice concentrations according to ERA-40 and ERA-Interim reanalysis data (Uppala et al., 2005; Dee et al., 2011; Berrisford et al., 2009). Every six hours the dynamic-thermodynamic state of the model atmosphere is constrained to observations by implicit nudging (e.g. Krishamurti

et al., 1991; implemented by Rast, 2008), i.e. modeled fields of surface pressure, temperature, divergence and vorticity are relaxed to ERA-40 and ERA-Interim reanalysis fields (Uppala et al., 2005; Dee et al., 2011; Berrisford et al., 2009; data have been obtained from the ECMWF data server). This approach ensures that the large-scale atmospheric flow is correctly represented also at the sub-seasonal time scale. The hydrological cycle in our ECHAM5 setup is fully prognostic and not nudged to reanalysis data. Our simulation starts on 1 September 1957 using an internal model time step of 12 min. Here, we evaluate daily averaged model results through 2010–2012.

In general, the model captures observed temperature and humidity trends in Bremen. Averaged over the years 2010–2012, the difference between modeled and observed daily surface temperatures is less than about $-1\,°C$. Averaged over the particular days with FTIR measurements, ECHAM5-wiso simulates surface temperatures which are about $3\,°C$ colder than the observations. Comparing simulated vertical temperature profiles with the NCEP a priori profiles used for isotope retrieval, we find that, averaged over the days with measurements, column-averaged temperatures according to ECHAM5-wiso are about $0.8\,°C$ colder than the a priori values. A similar comparison for specific humidity indicates that the total column water vapor simulated by ECHAM5-wiso is about 2 mm (or 26 %) higher than the a priori values according to NCEP. However, this moist bias tends to cancel in the retrieval when isotopic ratios are considered.

For comparison with FTIR, vertical profiles of $H_2^{16}O$, $H_2^{18}O$ and HDO from the model were vertically integrated to get total column values and then isotopic ratios were calculated.

4 Retrieval results and comparison with simulations

About 6000 spectra recorded from January 2010 to May 2012 at Bremen TCCON site were processed in order to retrieve columnar mean values of $\delta^{18}O$ and δD using the retrieval setup described above. Each spectral window of the species of interest (see Table 1) was processed independently and the results were filtered and averaged

N. V. Rokotyan et al.

with respect to uncertainty based on spectral residuals. Since GGG software uses NCEP/NCAR reanalysis data for vertical profiles of atmospheric temperatures interpolated to local noon for a whole day of measurements, we have used spectra recorded in a time range of local noon time ±3 h only. We removed from the comparison the days with measurements that cover less than 2 h. An offset correction was applied to the retrieval results in order to remove the shifts due to spectroscopic uncertainties (as described in Sect. 2.4).

While retrieval results from individual measurements are noisy, values averaged during one month of measurements show seasonal variability of δ^{18}O and δD of about 25 ‰ and 200 ‰ respectively. As expected, both δ^{18}O and δD generally follow atmospheric temperature. Correlation coefficient between δ^{18}O, δD and temperature at surface are 0.89 and 0.88 respectively while correlation coefficient between columnar δ^{18}O and δD is 0.86 (Fig. 8).

Figure 9 shows time-series of the retrieved "monthly" values of δ^{18}O and δD together with the output of ECHAM5-wiso general circulation model (Werner et al., 2011). Simulations and results retrieved from FTIR measurements are correlated with $r^2 = 0.81$ for δ^{18}O and $r^2 = 0.91$ for δD and scatter with an absolute standard deviation of 5.4 ‰ and 18.1 ‰ respectively. While retrieved value of δ^{18}O and δD show good agreement with the model, the precision of the retrieval must be improved to obtain useful deuterium excess values. Figure 10 shows scatter plots of the model vs. FTIR results. We define "summer" (red) and "winter" (blue) points corresponding to surface temperatures above 15 °C and below 15 °C respectively. "Summer" slope is equal to 0.74 and 0.79 for δ^{18}O and δD respectively, while "winter" slope values are 0.30 and 0.56. "Summer" results also show better r^2 values of 0.98 and 0.95 for δ^{18}O and δD, respectively. While "winter" r^2 values are much lower: 0.61 for δ^{18}O and 0.70 for δD. Possible reason of this change is incorrect temperature dependence of spectroscopic line parameters (as described in Sect. 2.4). This also explains why change in slope and correlation for δ^{18}O is higher than for δD because δD in the atmosphere is much more variable and spectroscopic uncertainties don't impact on the results so strongly.

5 Conclusions

We have analyzed the feasibility to estimate column-averaged atmospheric δ^{18}O and δD from ground-based high-resolution FTIR measurements in near IR. The method demonstrates the feasibility to retrieve seasonal variations of both δD and δ^{18}O. Time series of remotely measured δ^{18}O in the atmosphere are presented for the first time. Isotopic ratios retrieved from "summer" spectra show a good agreement with ECHAM5-wiso general circulation model, while the agreement with the retrieval from "winter" spectra is poor. A likely explanation of this behaviour is an incorrect definition of spectroscopic line parameters. Recent studies also report that Voigt line shape model does not describe the shape of water vapour absorption line perfectly (Boone et al., 2007; Schneider et al., 2011; Schneider and Hase, 2011) and usage of the speed-dependent Voigt model may improve the results, what is now difficult due to absence of speed-dependent Voigt spectroscopic data. Analysis of spectroscopic sources of the retrieval errors shows that there is potentiality to improve the method due to refinement of spectral line parameters because they produce main uncertainty in the retrieval results at present.

At this moment the precision of the method is not sufficient to obtain appropriate data for deuterium excess and further development of simultaneous remote atmospheric measurements of δ^{18}O and δD is particularly important for better understanding climate processes and atmospheric water cycle.

References

Anderson, G. P., Clough, S. A., Kneizys, F. X., Chetwynd, J. H., and Shettle, E. P.: AFGL atmospheric constituent profiles (0–120 km), AFGL-TR-0110, Environmentral Research Paper 954, Air Force Geophysics Laboratory, 43 pp., 1986.

5 Barber, R. J., Tennyson, J., Harris, G. J., and Tolchenov, R. N.: A high-accuracy computed water line list, Mon. Not. R. Astron. Soc., 368, 1087–1094, 2006.

Berrisford, P., Dee, D., Fielding, K., Fuentes, M., Kållberg, P., Kobayashi, S., and Uppala, S.: ERA report series – the ERA-Interim archive Version 1.0, 2009.

Boesch, H., Deutscher, N. M., Warneke, T., Byckling, K., Cogan, A. J., Griffith, D. W. T.,
10 Notholt, J., Parker, R. J., and Wang, Z.: HDO/H_2O ratio retrievals from GOSAT, Atmos. Meas. Tech., 6, 599–612, doi:10.5194/amt-6-599-2013, 2013.

Boone, C. D., Walker, K. A., and Bernath, P. F.: Speed-dependent Voigt profile for water vapor in infrared remote sensing applications, J. Quant. Spectrosc. Ra., 105, 525–532, doi:10.1016/j.jqsrt.2006.11.015, 2007.

15 Craig, H.: Standard for reporting concentrations of deuterium and oxygen-18 in natural waters, Science, 133, 1833–1834, 1961.

Coffey, M. T., Hannigan, J. W., and Goldman, A.: Observations of upper tropospheric/lower stratospheric water vapour and its isotopologues, J. Geophys. Res., 111, D14313, doi:10.1029/2005JD006093, 2006.

20 Coudert, L. H., Wagner, G., Birk, M., Baranov, Yu. I., Lafferty, W. J., and Flaud, J.-M.: The $H^{16}O$ molecule: line position and line 2 intensity analyses up to the second triad, J. Mol. Spectrosc., 251, 339–357, 2008.

Dansgaard, W.: Stable isotopes in precipitation, Tellus A, 16, 4, doi:10.3402/tellusa.v16i4.8993, 1964.

25 Dee, D. P., Uppala, S. M., Simmons, A. J., Berrisford, P., Poli, P., Kobayashi, S., Andrae, U., Balmaseda, M. A., Balsamo, G., Bauer, P., Bechtold, P., Beljaars, A. C. M., van de Berg, L., Bidlot, J., Bormann, N., Delsol, C., Dragani, R., Fuentes, M., Geer, A. J., Haimberger, L., Healy, S. B., Hersbach, H., Holm, E. V., Isaksen, L., Kallberg, P., Kohler, M., Matricardi, M., McNally, A. P., Monge-Sanz, B. M., Morcrette, J.-J., Park, B.-K., Peubey, C., de Rosnay, P.,
30 Tavolato, C., Thepaut, J.-N., and Vitart, F.: The ERA-Interim reanalysis: configuration and performance of the data assimilation system, Q. J. Roy. Meteorol. Soc., 137, 553–597, 2011.

Title Page

Abstract | Introduction

Conclusions | References

Tables | Figures

◄ | ►

◄ | ►

Back | Close

Full Screen / Esc

ECMWF data server: available at: http://data-portal.ecmwf.int/ (last access: 4 September 2013), 2013.

Frankenberg, C., Yoshimura, K., Warneke, T., Aben, I., Butz, A., Deutscher, N., Griffith, D., Hase, F., Notholt, J., Schneider, M., Schrijver, H., and Röckmann, T.: Dynamic processes governing lower-tropospheric HDO/H_2O ratios as observed from space and ground, Science, 325, 1374–1377, doi:10.1126/science.1173791, 2009.

Frankenberg, C., Wunch, D., Toon, G., Risi, C., Scheepmaker, R., Lee, J.-E., Wennberg, P., and Worden, J.: Water vapor isotopologue retrievals from high-resolution GOSAT shortwave infrared spectra, Atmos. Meas. Tech., 6, 263–274, doi:10.5194/amt-6-263-2013, 2013.

Gribanov, K. G. and Zakharov, V. I.: Possibility to monitor the HDO/H_2O content ratio in the atmosphere from space observations of the outgoing thermal radiation, Atmospheric and Ocean Optics, 12, 825–826, 1999.

Gribanov, K. G., Zakharov, V. I., and Tashkun, S. A.: FIRE-ARMS software package and its application to passive IR sensing of the atmosphere, Atmospheric and Ocean Optics, 12, 358–361, 1999.

Gribanov, K. G., Zakharov, V. I., Tashkun, S. A., and Tyuterev, V. G.: A new software tool for radiative transfer transfer calculations and its application to IMG/ADEOS data, J. Quant. Spectrosc. Ra., 68, 435–451, 2001.

Gribanov, K. G., Zakharov, V. I., Beresnev, S. A., Rokotyan, N. V., Poddubnyi, V. A, Imasu, R., Chistyakov, P. A., Skorik, G. G., and Vasin, V. V.: The sounding of HDO/H_2O in Ural's atmosphere using ground-based measurements of IR-solar radiation with high spectral resolution, Atmospheric and Ocean Optics, 24, 124–127, 2011.

Gribanov, K., Jouzel, J., Bastrikov, V., Bonne, J.-L., Breon, F.-M., Butzin, M., Cattani, O., Masson-Delmotte, V., Rokotyan, N., Werner, M., and Zakharov, V.: ECHAM5-wiso water vapour isotopologues simulation and its comparison with WS-CRDS measurements and retrievals from GOSAT and ground-based FTIR spectra in the atmosphere of Western Siberia, Atmos. Chem. Phys. Discuss., 13, 2599–2640, doi:10.5194/acpd-13-2599-2013, 2013.

Gryazin, V., Risi, C., Jouzel, J., Kurita, N., Worden, J., Frankenberg, C., Bastrikov, V., Gribanov, K., and Stukova, O.: The added value of water isotopic measurements for understanding model biases in simulating the water cycle over Western Siberia, Atmos. Chem. Phys. Discuss., submitted, 2013.

Hagemann, S., Arpe, K., and Roeckner, E.: Evaluation of the hydrological cycle in the ECHAM5 model, J. Climate, 19, 3810–3827, 2006.

Title Page

Abstract | Introduction

Conclusions | References

Tables | Figures

◄ | ►

◄ | ►

Back | Close

Full Screen / Esc

Printer-friendly Version

Interactive Discussion

Hannigan, J. W., Coffey, M. T., and Goldman, A.: Semi-autonomous FTS observation system for remote sensing of stratospheric and tropospheric gases, J. Atmos. Ocean Tech., 26, 1814–1828, doi:10.1175/2009JTECHA1230.1, 2009.

Herbin, H., Hurtmans, D., Turquety, S., Wespes, C., Barret, B., Hadji-Lazaro, J., Clerbaux, C., and Coheur, P.-F.: Global distributions of water vapour isotopologues retrieved from IMG/ADEOS data, Atmos. Chem. Phys., 7, 3957–3968, doi:10.5194/acp-7-3957-2007, 2007.

Herbin, H., Hurtmans, D., Clerbaux, C., Clarisse, L., and Coheur, P.-F.: $H_2^{16}O$ and HDO measurements with IASI/MetOp, Atmos. Chem. Phys., 9, 9433–9447, doi:10.5194/acp-9-9433-2009, 2009.

Hoffmann, G., Werner, M., and Heimann, M.: Water isotope module of the ECHAM atmospheric general circulation model: a study on timescales from days to several years, J. Geophys. Res., 103, 16871–16896, doi:10.1029/98JD00423, 1998.

Jenouvrier, A., Daumont, L., Regalia-Jarlot, L., Tyuterev, V. G., Carleer, M., Vandaele, A. C., Mikhailenko, S., and Fally, S.: Fourier transform measurements of water vapor line parameters in the 4200–6600 cm^{-1} region, J. Quant. Spectrosc. Ra., 105, 326–355, 2007.

Jouzel, J., Russel, G., Suozzo, R., Kloster, R., White, J., and Broecker, W.: Simulations of the HDO and $H_2^{18}O$ atmospheric cycles using the NASA GISS General Circulation Model: the seasonal cycle for present-day conditions, J. Geophys. Res., 92, 14739–14760, 1987.

Kalnay, E., Kanamitsu, M., Kistler, R., Collins, W., Deaven, D., Gandin, L., Iredell, M., Saha, S., White, G., Woollen, J., Zhu, Y., Leetmaa, A., Reynolds, R., Chelliah, M., Ebisuzaki, W., Higgins, W., Janowiak, J., Mo, K. C., Ropelewski, C., Wang, J., Jenne, R., and Joseph, D.: The NCEP/NCAR 40 yr reanalysis project, B. Am. Meteorol. Soc., 77, 437–471, 1996.

Keppel-Aleks, G., Toon, G. C., Wennberg, P. O., and Deutscher, N. M.: Reducing the impact of source brightness fluctuations on spectra obtained by Fourier-transform spectrometry, Appl. Optics, 46, 4774–4779, 2007.

Kerstel, E. R. T., van Trigt, R., Dam, N., Reuss, J., and Meijer, H. A. J.: Simultaneous determination of the $^2H/^1H$, $^{17}O/^{16}O$, and $^{18}O/^{16}O$, isotope abundance ratios in water by means of laser spectrometry, Anal. Chem., 71, 5297–5303, 1999.

Krishnamurti, T. N., Xue, J., Bedi, H. S., Ingles, K., and Oosterhof, D.: Physical initialization for numerical weather prediction over the tropics, Tellus A, 43, 53–81, doi:10.1034/j.1600-0870.1991.t01-3-00007.x, 1991.

Title Page

Abstract	Introduction
Conclusions	References
Tables	Figures

|◄ | ►|

◄ | ►

Back | Close

Full Screen / Esc

Printer-friendly Version

Interactive Discussion

Langebroeck, P. M., Werner, M., and Lohmann, G.: Climate information imprinted in oxygen-isotopic composition of precipitation in Europe, Earth Planet. Sc. Lett., 311, 144–154, 2011.

Lee, X., Sargent, S., Smith, R., and Tanner, B.: In situ measurement of the water vapor o-18/o-16 isotope ratio for atmospheric and ecological applications, J. Atmos. Ocean. Tech., 22, 1305–1305, doi:10.1175/JTECH9001.1a, 2005.

Merlivat, L. and Jouzel, J.: Global climatic interpretation of the deuterium-oxygen 18 relationship for precipitation, J. Geophys. Res., 84, 5029, doi:10.1029/JC084iC08p05029, 1979.

Mikhailenko, S. N., Le, W., Kassi, S., and Campargue, A.: Weak water absorption lines around 1.455 and 1.66 μm by CW-CRDS, J. Mol. Spectrosc., 244/2, 170–178, 2007.

Mikhailenko, S. N., Albert, K. A. K., Mellau, G., Klee, S., Winnewisser, B. P., Winnewisser, M., and Tyuterev, V. G.: Water vapor absorption line intensities in the 1900–6600 cm^{-1} region, J. Quant. Spectrosc. Ra., 109, 2687–2696, 2008.

Moyer, E. J., Irion, F. W., Yung, Y. L., and Gunson, M. R.: ATMOS stratospheric deuterated water and implications for troposphere stratosphere transport, Geophys. Res. Lett., 23, 2385–2388, 1996.

Noone, D. and Simmonds, I.: Associations between delta O-18 of water and climate parameters in a simulation of atmospheric circulation for 1979–95, J. Climate, 15, 3150–3169, 2002.

Pommier, M., Lacour, J.-L., Risi, C., Bréon, F.-M., Clerbaux, C., Coheur, P.-F., Gribanov, K., Hurtmans, D., Jouzel, J., and Zakharov, V.: Observation of tropospheric δD by IASI over the Western Siberia: comparison with a GCM, Atmos. Meas. Tech. Discuss., 6, 11055–11092, doi:10.5194/amtd-6-11055-2013, 2013.

Payne, V. H., Noone, D., Dudhia, A., Piccolo, C., and Grainger, R. G.: Global satellite measurements of HDO and implications for understanding the transport of water vapour into the stratosphere, Q. J. Roy. Meteor. Soc., 133, 1459–1471, doi:10.1002/qj.127, 2007.

Rast, S.: Sea ice and nudging in ECHAM5, available at: http://www.mpimet.mpg.de/en/staff/sebastian-rast/echam-special-documentation.html (last access: 10 January 2014), 2008.

Rinsland, C. P., Gunson, M. R., Foster, J. C., Toth, R. A., Farmer, C. B., and Zander, R.: Stratospheric profiles of heavy water vapor isotopes and CH_3D from Analysis of the ATMOS Spacelab 3 infrared solar spectra, J. Geophys. Res., 96, 1057–1068, 1991.

Risi, C., Bony, S., Vimeux, F., and Jouzel, J.: Water-stable isotopes in the LMDZ4 general circulation model: model evaluation for present-day and past climates and applications to climatic interpretations of tropical isotopic records, J. Geophys. Res., 115, 1–27, doi:10.1029/2009JD013255, 2010a.

Title Page

Abstract | Introduction

Conclusions | References

Tables | Figures

◄ | ►

◄ | ►

Back | Close

Full Screen / Esc

Printer-friendly Version

Interactive Discussion

Risi, C., Bony, S., Vimeux, F., Frankenberg, C., Noone, D., and Worden, J.: Understanding the Sahelian water budget through the isotopic composition of water vapor and precipitation, J. Geophys. Res., 115, D24110, doi:10.1029/2010JD014690, 2010b.

Risi, C., Noone, D., Worden, J., Frankenberg, C., Stiller, G., Kiefer, M., Funke, B., Walker, K., Bernath, P., Schneider, M., Wunch, D., Sherlock, V., Deutscher, N., Griffith, D., Wennberg, P. O., Strong, K., Smale, D., Mahieu, E., Barthlott, S., Hase, F., García, O., Notholt, J., Warneke, T., Toon, G., Sayres, D., Bony, S., Lee, J., Brown, D., Uemura, R., and Sturm, C.: Process-evaluation of tropospheric humidity simulated by general circulation models using water vapor isotopologues: 1. Comparison between models and observations, J. Geophys. Res., 117, D05303, doi:10.1029/2011JD016621, 2012a.

Risi, C., Noone, D., Worden, J., Frankenberg, C., Stiller, G., Kiefer, M., Funke, B., Walker, K., Bernath, P., Schneider, M., Bony, S., Lee, J., Brown, D., and Sturm, C.: Process-evaluation of tropospheric humidity simulated by general circulation models using water vapor isotopic observations: 2. Using isotopic diagnostics to understand the mid and upper tropospheric moist bias in the tropics and subtropics, J. Geophys. Res., 117, D05304, doi:10.1029/2011JD016623, 2012b.

Risi, C., Noone, D., Frankenberg, C., and Worden, J.: Role of continental recycling in intraseasonal variations of continental moisture as deduced from model simulations and water vapor isotopic measurements, Water Resour. Res., 49, 1–21, doi:10.1002/wrcr.20312, 2013.

Rodgers, C. D.: Inverse Methods for Atmospheric Sounding: Theory and Practice, World Scientific, 2000.

Rothman, L. S., Gordon, I. E., Barbe, A., Benner, D. C., Bernath, P. F., Birk, M., Boudon, V., Brown, L. R., Campargue, A., and Champion, J. P.: The HITRAN 2008 molecular spectroscopic database, J. Quant. Spectrosc. Ra., 110, 533–572, doi:10.1016/j.jqsrt.2009.02.013, 2009.

Rothman, L. S., Gordon, I. E., Babikov, Y., Barbe, A., Benner, D. C., Bernath, P. F., Birk, M., Bizzocchi, L., Boudon, V., Brown, L. R., Campargue, A., Chance, K., Coudert, L. H., Devi, V. M., Drouin, B. J., Fayt, A., Flaud, J.-M., Gamache, R. R., Harrison, J., Hartmann, J.-M., Hill, C., Hodges, J. T., Jacquemart, D., Jolly, A., Lamouroux, J., LeRoy, R. J., Li, G., Long, D., Mackie, C. J., Massie, S. T., Mikhailenko, S., Müller, H. S. P., Naumenko, O. V., Nikitin, A. V., Orphal, J., Perevalov, V. I., Perrin, A., Polovtseva, E. R., Richard, C., Smith, M. A. H., Starikova, E., Sung, K, Tashkun, S. A., Tennyson, J., Toon, G. C., Tyuterev, Vl. G., and Wag-

Title Page

Abstract | Introduction

Conclusions | References

Tables | Figures

|◄ | ►|

◄ | ►

Back | Close

Full Screen / Esc

Printer-friendly Version

Interactive Discussion

ner, G.: The HITRAN 2012 Molecular Spectroscopic Database, J. Quant. Spectrosc. Ra., Elsevier, ISSN 0022-4073, 2013.

Roeckner, E., Bäuml, G., Bonaventura, L. Brokopf, R., Esch, M., Giorgetta, M., Hagemann, S., Kirchner, I., Kornblueh, L., Manzini, E., Rhodin, A., Schlese, U., Schulzweida, U., and Tompkins, A.: The atmospheric general circulation model ECHAM5, Part 1, Model description, Report No. 349, Max Planck Institute for Meteorology, Hamburg, Germany, 2003.

Roeckner, E., Brokopf, R., Esch, M., Giorgetta, M., Hagemann, S., Manzini, E., Schlese, U., and Schulzweida, U.: Sensitivity of simulated climate to horizontal and vertical resolution in the ECHAM5 atmosphere model, J. Climate, 19, 3771–3791, 2006.

Rozanski, K., Araguás-Araguás, L., and Gonfiantini, R.: Relation between long-term trends of oxygen-18 isotope composition of precipitation and climate, Science, 258, 981–985, 1992.

Shillings, A. J. L., Ball, S. M., Barber, M. J., Tennyson, J., and Jones, R. L.: An upper limit for water dimer absorption in the 750 nm spectral region and a revised water line list, Atmos. Chem. Phys., 11, 4273–4287, doi:10.5194/acp-11-4273-2011, 2011.

Schneider, M. and Hase, F.: Optimal estimation of tropospheric H_2O and δD with IASI/METOP, Atmos. Chem. Phys., 11, 11207–11220, doi:10.5194/acp-11-11207-2011, 2011.

Schneider, M., Hase, F., and Blumenstock, T.: Ground-based remote sensing of HDO/H_2O ratio profiles: introduction and validation of an innovative retrieval approach, Atmos. Chem. Phys., 6, 4705–4722, doi:10.5194/acp-6-4705-2006, 2006.

Schneider, M., Toon, G. C., Blavier, J.-F., Hase, F., and Leblanc, T.: H_2O and δD profiles remotely-sensed from ground in different spectral infrared regions, Atmos. Meas. Tech., 3, 1599–1613, doi:10.5194/amt-3-1599-2010, 2010.

Schneider, M., Hase, F., Blavier, J. F., Toon, G. C., and Leblanc, T.: An empirical study on the importance of a speed-dependent Voigt line shape model for tropospheric water vapor profile remote sensing, J. Quant. Spectrosc. Ra., 112, 465–474, doi:10.1016/j.jqsrt.2010.09.008, 2011.

Schneider, M., Barthlott, S., Hase, F., González, Y., Yoshimura, K., García, O. E., Sepúlveda, E., Gomez-Pelaez, A., Gisi, M., Kohlhepp, R., Dohe, S., Blumenstock, T., Wiegele, A., Christner, E., Strong, K., Weaver, D., Palm, M., Deutscher, N. M., Warneke, T., Notholt, J., Lejeune, B., Demoulin, P., Jones, N., Griffith, D. W. T., Smale, D., and Robinson, J.: Ground-based remote sensing of tropospheric water vapour isotopologues within the project MUSICA, Atmos. Meas. Tech., 5, 3007–3027, doi:10.5194/amt-5-3007-2012, 2012.

Skorik, G. G., Vasin, V. V., Gribanov, K. G., Jouze, L. J., Zakharov, V. I., and Rokotyan, N. V.: Retrieval of vertical profiles of water vapour isotopologues in the atmosphere using infrared transmission spectra of solar radiation, Academy of Science Reports, in press, 2014.

Steen-Larsen, H. C., Johnsen, S. J., Masson-Delmotte, V., Stenni, B., Risi, C., Sodemann, H., Balslev-Clausen, D., Blunier, T., Dahl-Jensen, D., Ellehøj, M. D., Falourd, S., Grindsted, A., Gkinis, V., Jouzel, J., Popp, T., Sheldon, S., Simonsen, S. B., Sjolte, J., Steffensen, J. P., Sperlich, P., Sveinbjörnsdóttir, A. E., Vinther, B. M., and White, J. W. C.: Continuous monitoring of summer surface water vapor isotopic composition above the Greenland Ice Sheet, Atmos. Chem. Phys., 13, 4815–4828, doi:10.5194/acp-13-4815-2013, 2013.

Tolchenov, R. and Tennyson, J.: Water line parameters from refitted spectra constrained by empirical upper state levels: study of the 9500–14500 cm^{-1} region, J. Quant. Spectrosc. Ra., 109, 559–568, doi:10.1016/j.jqsrt.2007.08.001, 2008.

Uppala, S. M., Kållberg, P. W., Simmons, A. J., Andrae, U., da Costa Bechtold, V., Fiorino, M., Gibson, J. K., Haseler, J., Hernandez, A., Kelly, G. A., Li, X., Onogi, K., Saarinen, S., Sokka, N., Allan, R. P., Andersson, E., Arpe, K., Balmaseda, M. A., Beljaars, A. C. M., van de Berg, L., Bidlot, J., Bormann, N., Caires, S., Chevallier, F., Dethof, A., Dragosavac, M., Fisher, M., Fuentes, M., Hagemann, S., Hólm, E., Hoskins, B. J., Isaksen, L., Janssen, P. A. E. M., Jenne, R., McNally, A. P., Mahfouf, J.-F., Morcrette, J.-J., Rayner, N. A., Saunders, R. W., Simon, P., Sterl, A., Trenberth, K. E., Untch, A., Vasiljevic, D., Viterbo, P., and Woollen, J. 2005: The ERA-40 re-analysis, Q. J. Roy. Meteorol. Soc., 131, 2961–3012, 2005.

Werner, M., Heimann, M., and Hoffmann, G.: Isotopic composition and origin of polar precipitation in present and glacial climate simulations, Tellus B, 53, 53–71, 2001.

Werner, M., Langebroek, P. M., Carlsen, T., Herold, M., and Lohmann, G.: Stable water isotopes in the ECHAM5 general circulation model: toward highresolution isotope modeling on a global scale, J. Geophys. Res., 16, D15109, doi:10.1029/2011JD015681, 2011.

Worden, J., Bowman, K., Noone, D., Beer, R., Clough, S., Eldering, A., Fisher, B., Goldman, A., Gunson, M., Herman, R., Kulawik, S. S., Lampel, M., Luo, M., Osterman, G., Rinsland, C., Rodgers, C., Sander, S., Shephard, M., and Worden, H.: Tropospheric emission spectrometer observations of the tropospheric HDO/H$_2$O ratio: estimation approach and characterization, J. Geophys. Res., 111, D16309, doi:10.1029/2005JD006606, 2006.

Worden, J., Noone, D., Bowman, K., Beer, R., Eldering, A., Fisher, B., Gunson, M., Goldman, A., Herman, R., Kulawik, S. S., Lampel, M., Osterman, G., Rinsland, C., Rodgers, C., Sander, C.,

Title Page

Abstract | Introduction

Conclusions | References

Tables | Figures

|◄ | ►|

◄ | ►

Back | Close

Full Screen / Esc

Printer-friendly Version

Interactive Discussion

Shephard, M., Webster, C. R., and Worden, H.: Importance of rain evaporation and continental convection in the tropical water cycle, Nature, 445, 528–532, doi:10.1038/nature05508, 2007.

Wunch, D., Toon, G. C., Wennberg, P. O., Wofsy, S. C., Stephens, B. B., Fischer, M. L., Uchino, O., Abshire, J. B., Bernath, P., Biraud, S. C., Blavier, J.-F. L., Boone, C., Bowman, K. P., Browell, E. V., Campos, T., Connor, B. J., Daube, B. C., Deutscher, N. M., Diao, M., Elkins, J. W., Gerbig, C., Gottlieb, E., Griffith, D. W. T., Hurst, D. F., Jiménez, R., Keppel-Aleks, G., Kort, E. A., Macatangay, R., Machida, T., Matsueda, H., Moore, F., Morino, I., Park, S., Robinson, J., Roehl, C. M., Sawa, Y., Sherlock, V., Sweeney, C., Tanaka, T., and Zondlo, M. A.: Calibration of the Total Carbon Column Observing Network using aircraft profile data, Atmos. Meas. Tech., 3, 1351–1362, doi:10.5194/amt-3-1351-2010, 2010.

Wunch, D., Toon, G. C., Blavier, J.-F. L., Washenfelder, R. A., Notholt, J., Connor, B. J., Griffith, D. W. T., Sherlock, V., and Wennberg, P. O.: The total carbon column observing network, Philos. T. R. Soc. A, 369, 2087–2112, 2011.

Yoshimura, K., Kanamitsu, M., Noone, D., and Oki, T.: Historical isotope simulation using reanalysis atmospheric data, J. Geophys. Res., 113, 1–15, doi:10.1029/2008JD010074, 2008.

Zakharov, V. I., Imasu, R., Gribanov, K. G., Hoffmann, G., and Jouzel, J.: Latitudinal distribution of the deuterium to hydrogen ratio in the atmospheric water vapor retrieved from IMG/ADEOS data, Geophys. Res. Lett., 31, L12104, doi:10.1029/2004GL019433, 2004.

Table 1. Summarized information about spectral windows used for the retrieval of $\delta^{18}O$ and δD. Windows marked by "$*$" are used in TCCON community.

Molecule	Center, cm^{-1}	Width, cm^{-1}	Interfering Species	
$H_2^{18}O$	4056.50	1.0	$H_2^{16}O$ CO_2 CH_4	
$H_2^{18}O$	4062.75	1.0	$H_2^{16}O$ CO_2 CH_4	
$H_2^{18}O$	4067.50	2.0	$H_2^{16}O$ CO_2 CH_4	
$H_2^{18}O$	4090.50	1.0	$H_2^{16}O$ CO_2 CH_4	
$H_2^{18}O$	4115.25	1.5	$H_2^{16}O$ CO_2 CH_4	
$H_2^{18}O$	5012.25	1.5	$H_2^{16}O$ CO_2 CH_4	
$H_2^{18}O$	5076.90	0.6	$H_2^{16}O$ CO_2 CH_4	
$H_2^{18}O$	6656.25	1.0	$H_2^{16}O$ CO_2 CH_4	
$H_2^{18}O$	6739.30	2.5	$H_2^{16}O$ $H_2^{17}O$	
$H_2^{18}O$	6740.20	1.0	$H_2^{16}O$ $H_2^{17}O$	
$H_2^{18}O$	6772.40	0.7	$H_2^{16}O$ HDO	
$H_2^{18}O$	6845.00	2.5	$H_2^{16}O$ CO_2 CH_4	
$H_2^{18}O$	6858.00	2.0	$H_2^{16}O$ CO_2 CH_4	
$H_2^{18}O$	6889.50	1.5	$H_2^{16}O$ CO_2 CH_4	
$H_2^{18}O$	6927.50	1.5	$H_2^{16}O$ CO_2 CH_4	
$H_2^{18}O$	7030.00	2.0	$H_2^{16}O$ CO_2 CH_4	
HDO	4038.00	2.0	$H_2^{16}O$ HF OCS O_3	
HDO	4054.60	3.3	$H_2^{16}O$ CH_4	$*$
HDO	4100.36	0.9	$H_2^{16}O$ CH_4 OCS	
HDO	4116.10	8.0	$H_2^{16}O$ OCS	$*$
HDO	4144.50	0.8	$H_2^{16}O$ CH_4	
HDO	4157.70	1.2	$H_2^{16}O$ CH_4	
HDO	4212.45	1.9	$H_2^{16}O$ CH_4	$*$
HDO	4232.50	11.0	$H_2^{16}O$ CH_4	$*$
HDO	5058.95	0.6	$H_2^{16}O$ CO_2	
HDO	6330.05	45.5	$H_2^{16}O$ CO_2	$*$
HDO	6377.40	50.2	$H_2^{16}O$ CO_2	$*$
$H_2^{16}O$	4259.57	1.0	HDO CH_4	
$H_2^{16}O$	4504.98	1.0	CH_4	
$H_2^{16}O$	4514.00	6.0	CH_4	
$H_2^{16}O$	4523.50	2.0	CH_4	
$H_2^{16}O$	4546.87	1.0	CH_4	

Table 1. Continued.

Molecule	Center, cm^{-1}	Width, cm^{-1}	Interfering Species	
H$_2^{16}$O	4552.00	2.5	CH$_4$	
H$_2^{16}$O	4556.20	2.0	CH$_4$	
H$_2^{16}$O	4565.20	2.5	CO$_2$ CH$_4$	*
H$_2^{16}$O	4571.75	2.5	CO$_2$ CH$_4$	*
H$_2^{16}$O	4576.85	1.9	CH$_4$	*
H$_2^{16}$O	4601.77	1.0	CO$_2$ CH$_4$	
H$_2^{16}$O	4609.45	1.0	CO$_2$ CH$_4$	
H$_2^{16}$O	4611.05	2.2	CH$_4$	*
H$_2^{16}$O	4622.00	2.3	CO$_2$	*
H$_2^{16}$O	4635.00	10.0	CO$_2$ CH$_4$	
H$_2^{16}$O	4645.00	10.0	CO$_2$ CH$_4$	
H$_2^{16}$O	4655.00	10.0	CO$_2$ CH$_4$	
H$_2^{16}$O	4681.93	1.0		
H$_2^{16}$O	4699.55	4.0	N$_2$O	*
H$_2^{16}$O	4706.43	1.0		
H$_2^{16}$O	4811.56	1.0	CO$_2$	
H$_2^{16}$O	4848.03	1.0	CO$_2$	
H$_2^{16}$O	4893.14	1.0	CO$_2$	
H$_2^{16}$O	5056.98	1.0	CO$_2$ HDO	
H$_2^{16}$O	5084.27	1.0	H$_2^{18}$O CO$_2$	
H$_2^{16}$O	5619.16	1.0		
H$_2^{16}$O	5696.16	1.0	CH$_4$	
H$_2^{16}$O	5741.13	1.0	CH$_4$	
H$_2^{16}$O	6034.2	1.7	CO$_2$ CH$_4$	
H$_2^{16}$O	6047.79	1.0	CO$_2$	
H$_2^{16}$O	6076.90	3.85	HDO CO$_2$ CH$_4$	*
H$_2^{16}$O	6099.35	1.0	CO$_2$	*
H$_2^{16}$O	6125.85	1.5	CO$_2$ CH$_4$	*
H$_2^{16}$O	6177.30	0.8	CO$_2$ CH$_4$	*
H$_2^{16}$O	6185.68	1.0	HDO CO$_2$ CH$_4$	
H$_2^{16}$O	6255.95	3.6	HDO CO$_2$	*
H$_2^{16}$O	6301.35	7.9	HDO CO$_2$	*
H$_2^{16}$O	6392.45	3.1	HDO	*
H$_2^{16}$O	6401.15	1.2	HDO	*
H$_2^{16}$O	6469.60	3.5	HDO CO$_2$	*
H$_2^{16}$O	6486.52	1.0	HDO CO$_2$	
H$_2^{16}$O	6604.51	1.0		

Title Page

Abstract | Introduction

Conclusions | References

Tables | Figures

|◄ | ►|

◄ | ►

Back | Close

Full Screen / Esc

Printer-friendly Version

Interactive Discussion

Fig. 1. Example of retrieved a priori guess scaling factors for refined $H_2^{18}O$ windows. Values from different windows are shifted relative to each other due to spectroscopic lines intensity and half-width uncertainties.
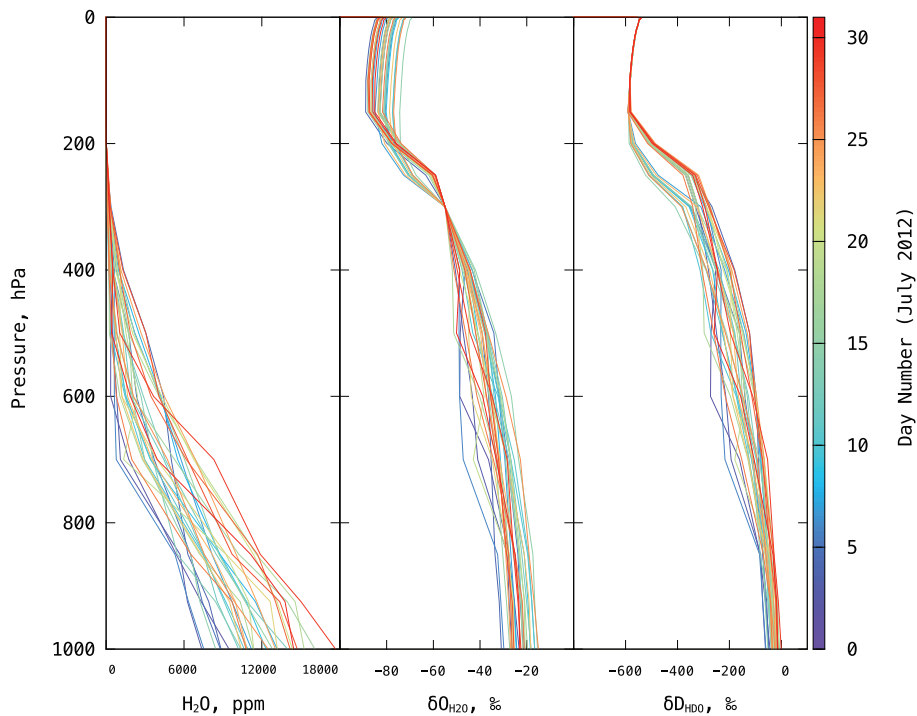
Title Page

Abstract | Introduction

Conclusions | References

Tables | Figures

◀◀ | ▶▶

◀ | ▶

Back | Close

Full Screen / Esc

Printer-friendly Version

Interactive Discussion
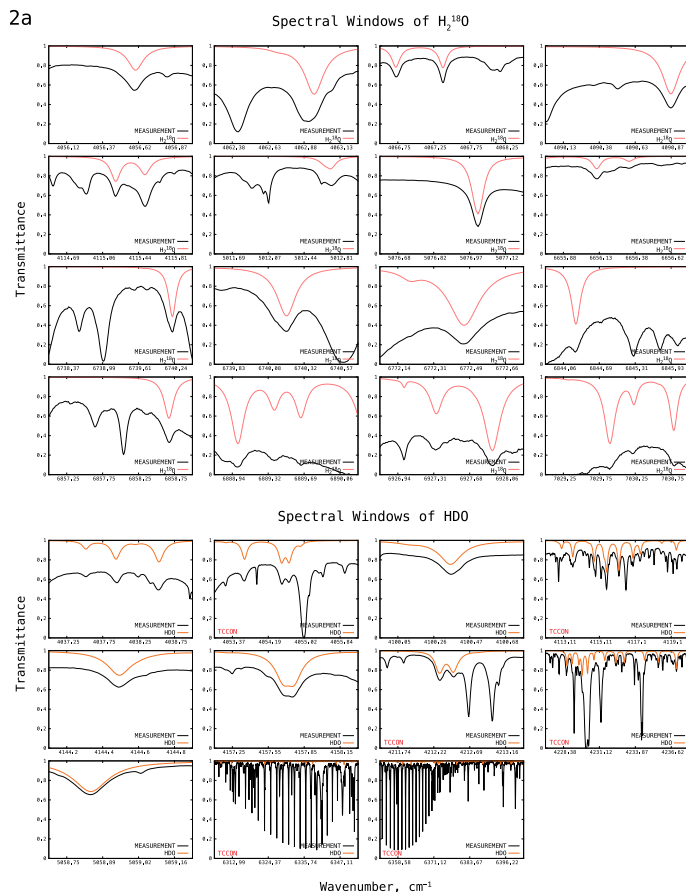
Fig. 2a. Refined set of spectral windows for $H_2^{18}O$ and HDO retrieval. Black line: measurement; red and orange lines: signals of $H_2^{18}O$ and HDO respectively. "TCCON" inscription indicates spectral windows used by TCCON community.

Title Page

Abstract | Introduction

Conclusions | References

Tables | Figures

◄ | ►|

◄ | ►

Back | Close

Full Screen / Esc

Printer-friendly Version

Interactive Discussion

2b

Spectral windows of $H_2^{16}O$
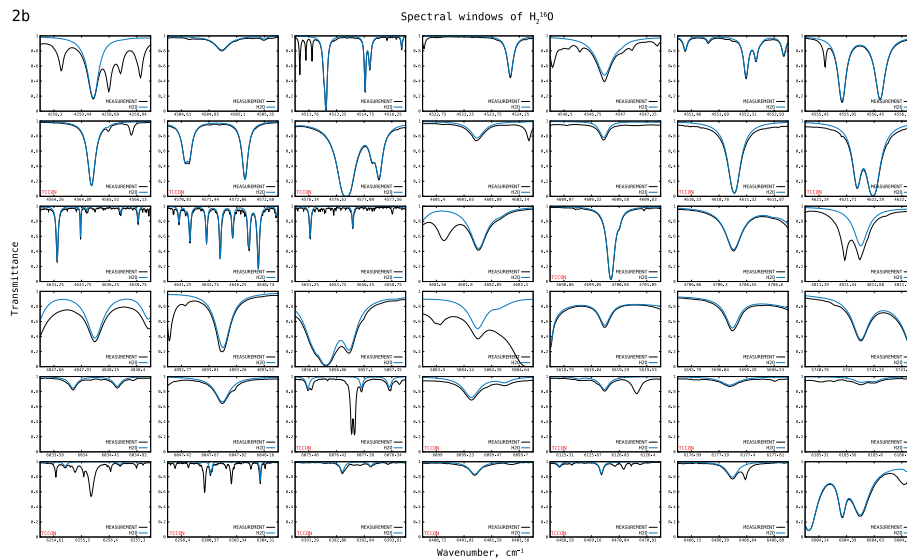
Fig. 2b. The same as Fig. 2a, but for $H_2^{16}O$.
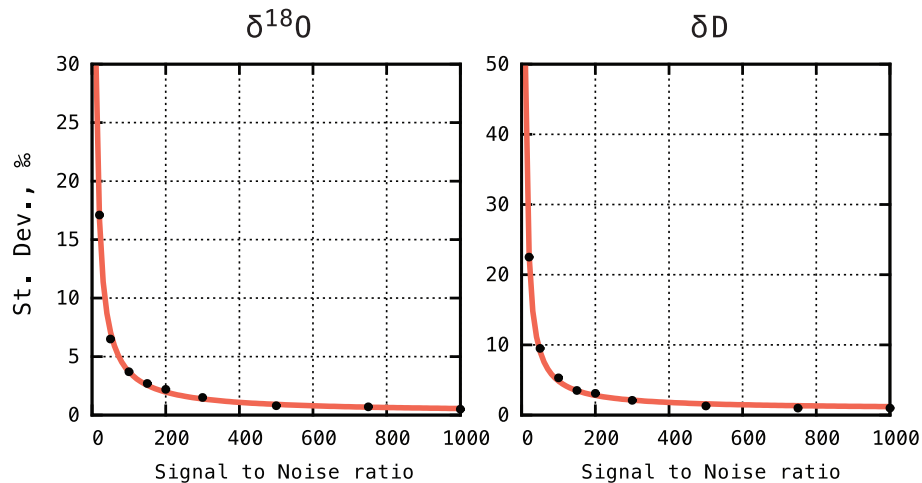
Fig. 3. Precision of the retrieval as a function of the signal to noise ratio of the measurement.
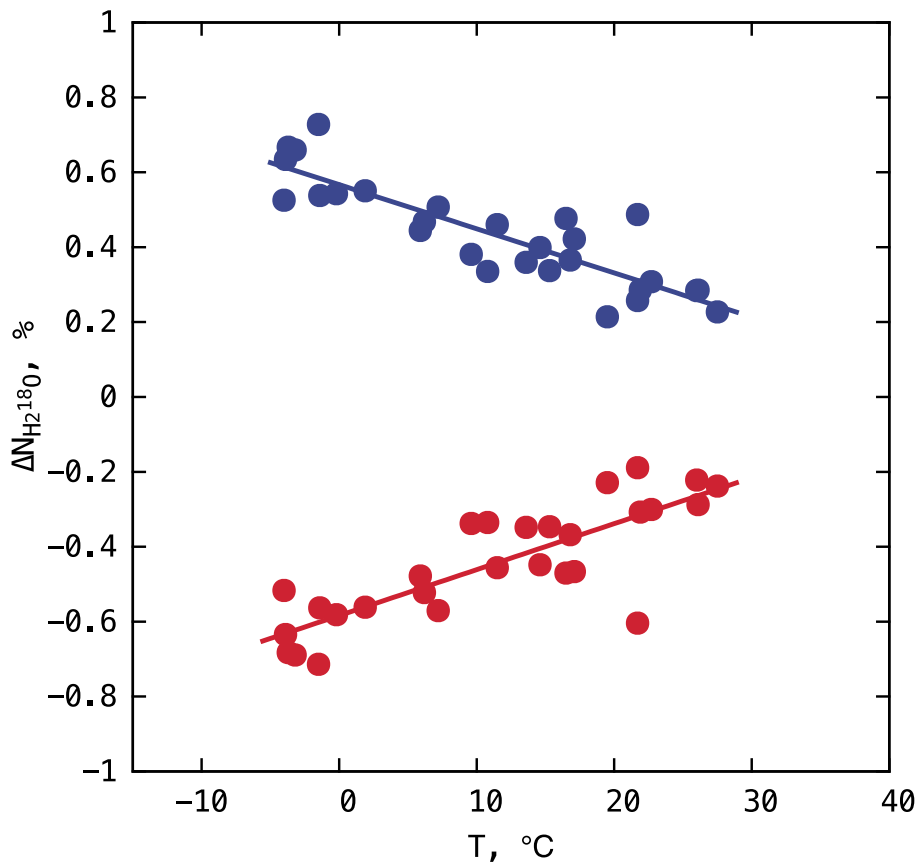
Fig. 4. Change in $H_2^{18}O$ concentration due to change in coefficient of temperature dependence of air-broadened half width by 0.85 (red dots) and 1.15 (blue dots).
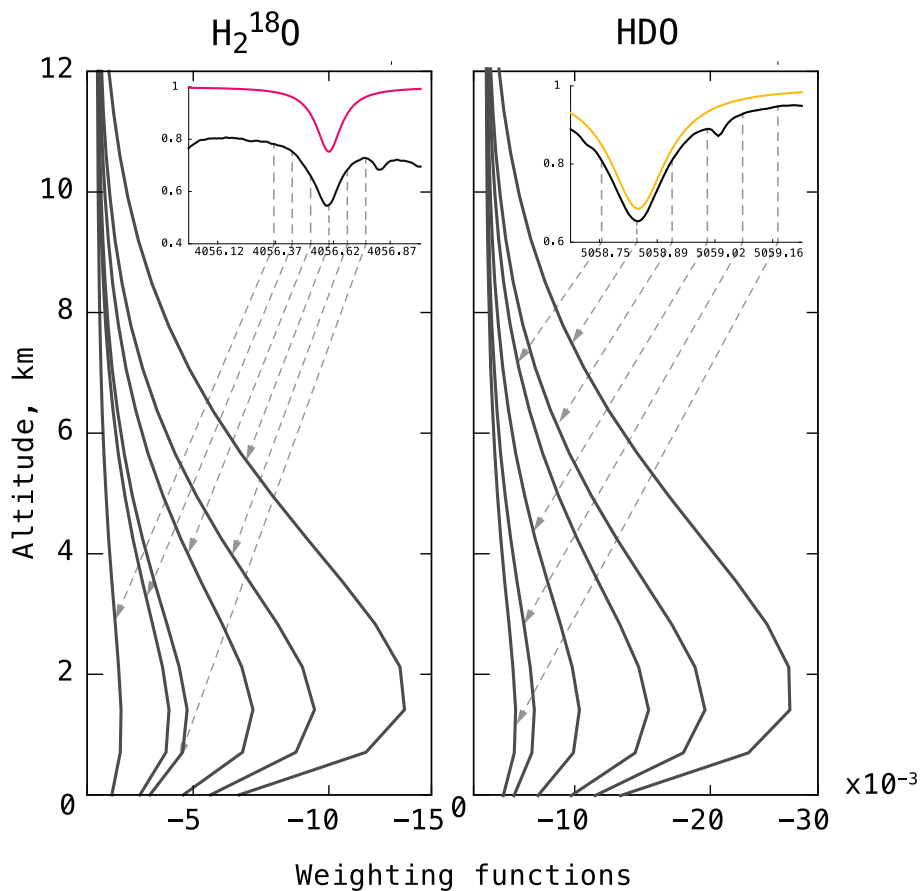
Fig. 5. Example of weighting functions of H$_2^{18}$O and HDO.

Fig. 6. Example of H_2O, δO_{H_2O} and δD_{HDO} initial guess profiles derived from NCEP/NCAR reanalysis data.
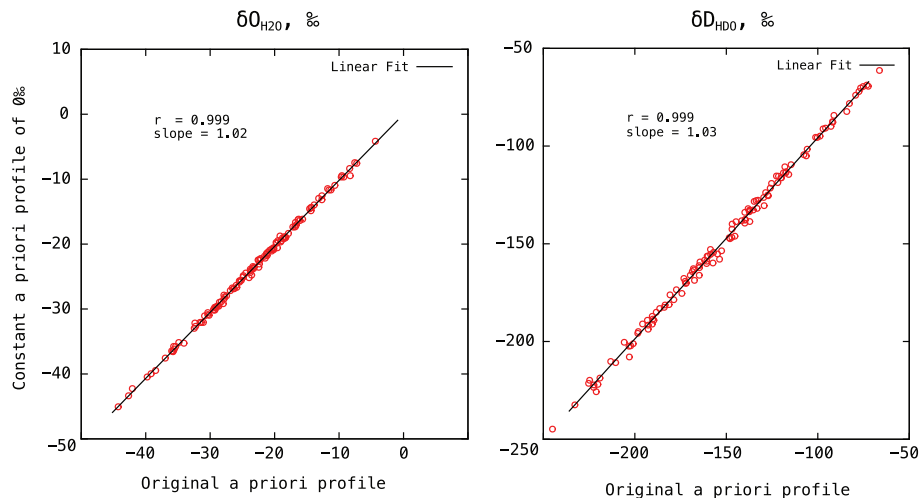
Fig. 7. Sensitivity of the retrieval to a priori assumptions. Results obtained using constant $\delta^{18}O$ and δD profiles of 0‰ vs. results obtained with $H_2^{18}O$ and HDO a priori profiles approximated by Eqs. (3) and (4).
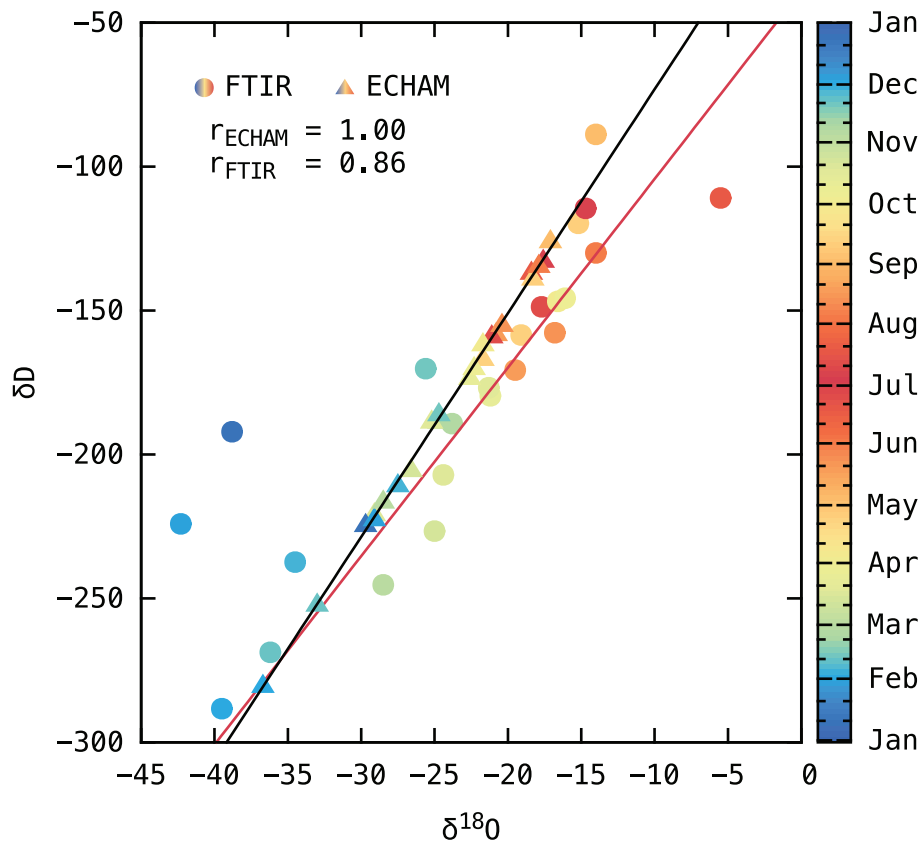
Fig. 8. Scatter plot of the retrieved (color dots) and simulated (color triangles) columnar values of $\delta^{18}O$ and δD.

Discussion Paper | Discussion Paper | Discussion Paper | Discussion Paper

Fig. 9. Retrieved values of δ^{18}O, δD and d-excess averaged during each month of measurements and corresponding ECHAM5-wiso model values.
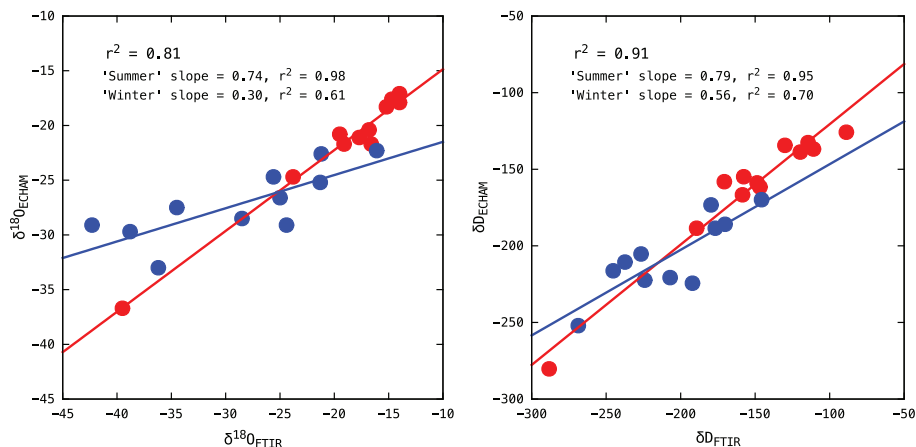
Fig. 10. Correlation between retrieved δ^{18}O and δD and ECHAM5-wiso model values. "Summer" red points correspond to surface air temperatures above 15 °C, "winter" blue points correspond to temperatures below 15 °C.